Polarization Holographic Recording in Amorphous Polymer with Photoinduced Linear and Circular Birefringence

Gabriella Cipparrone,*,† Pasquale Pagliusi,† Clementina Provenzano,† and Valery P. Shibaev‡

IPCF-CNR, UOS Cosenza, Excellence Centre CEMIF.CAL and Physics Department, University of Calabria, Ponte P. Bucci, Cubo 33B, 87036 Rende-CS, Italy, and Chemistry Department, M. V. Lomonosov Moscow State University, Moscow, 119991, Russia

Received: April 29, 2010

Polarization grating recording in an amorphous and nonchiral azo copolymer has been investigated. The reported study shows that the amorphous polymeric film undergoes a light-guided inhomogeneous supramolecular modification as a consequence of the illumination with proper polarized light patterns, acquiring new functionalities. Both linear and circular, spatially modulated, photoinduced birefringences occur, attaining their peak values in the linearly and circularly polarized regions of the light pattern, respectively. The photoinduced anisotropic structures strongly affect the polarization state of the light propagating through them, and the characterization of their optical diffraction enables measurement of the amplitude of the linear and circular birefringences. The recorded gratings show long-time stability and full reconfigurability functional to the multiple holographic recording.

Introduction

Polarization holographic recording techniques have attracted special attention because of their ability to create several optical polarization patterns.[1] The polarization gratings, obtained by applying these holographic methods, are commonly described as periodic spatial modulations in the (linear and/or circular) optical anisotropies of the exploited photosensitive materials. Contrary to the conventional phase or amplitude gratings, they operate by locally modifying the polarization state of light waves passing through them. This enables one to develop highly functionalized optical devices, able to control the beam propagation and the polarization state, useful for holographic data storage and display technology.[1]

Recently, several studies and strategies were addressed toward the supramolecular approach permitting to manipulate the local molecular environment of the organic materials for photonics, electrooptics, and nanotechnologies. They make it possible to obtain the molecular architectures at different length scales, providing several advantages for creation of a new generation of materials with increasing functionalities.[2−4] One intriguing possibility is to exploit the light that, due to its features and depending on the peculiarities of the materials, enables induction of molecular orientation and to create chiral structures as well as to cause surface structural patterns formation.

At the present time, photosensitive or photoresponsive materials are extensively being investigated as photocontrollable organized systems.[5−26] It is well-known that azobenzene-containing materials including polymers can easily undergo axis-selective *trans*−*cis*−*trans* photoisomerization and subsequent orientation of the azobenzene groups, if irradiated with linearly polarized light, resulting in a photoinduced linear birefringence.[5−15] Moreover, exploiting circularly or elliptically polarized light, photoinduced chirality has been demonstrated in azobenzene polymers, at both the molecular and the supramolecular levels.[16−26]

The authors of the present paper have recently investigated amorphous, nonchiral azo-polymers with peculiar light-controlled functionalities and good performance for optical data storage.[26−28] Beside the linear photoinduced birefringence (usual for azo-compounds), supramolecular chiral structures, whose handedness depends on the helicity of the light, were also photoinduced in the polymer films after irradiation with a circularly polarized light beam. These structures strongly affect the polarization state of the light propagating through the sample. In particular, the conversion from circular toward linear polarization and the simultaneous self-induced rotation of the major axis of the ellipse have been observed during the irradiation, which demonstrate that optical activity has been induced in the material. Because of the memory effect, the system preserves the imprinted chiral features for several months or even longer; nevertheless, they can be managed, controlling the exposure time or even via successive irradiations. A full reconfigurability is guaranteed by the intrinsic reversibility of the photoinduced processes.[27,28] The features and the performances of the photoinduced processes are unique with respect to similar published works in which liquid crystalline azobenzene polymers or preoriented amorphous copolymers have been investigated.[19−25] Additionally, high sensitivity, spatial resolution, time stability, full reconfigurability, and good performance of multiple hologram recording for one of amorphous azopolymers have also been demonstrated, making it attractive for holographic recording and high-density data storage.[28]

In the present paper, we study the capabilities and the performances of an amorphous, nonchiral azo-polymer film, in the polarization holographic recording, where light patterns with periodically modulated polarization may induce both linear and circular anisotropies. Two polarization configurations have been investigated, generated by the interference of two recording plane waves with orthogonal linear polarization, oriented at

* To whom correspondence should be addressed. Tel: +39-0984-496148. Fax: +39-0984-494401. E-mail: gabriella.cipparrone@fis.unical.it.
† University of Calabria.
‡ Moscow State University.

10.1021/jp103899b
Published on Web 06/22/2010

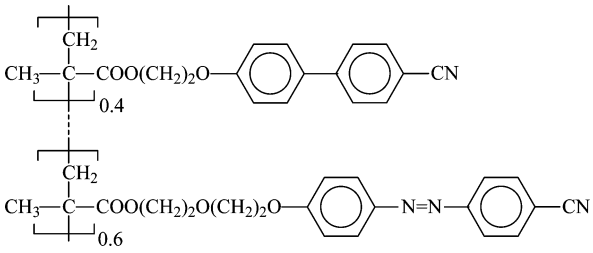

Figure 1. Structure of the side chain polymethacrylic copolymer.

±45° and 0°/90° with respect to the grating vector, respectively. The resulting light fields in the interference region are characterized by an almost uniform intensity distribution, while the polarization state periodically varies from linear to elliptical, circular, orthogonal elliptical, orthogonal linear, and so on. The stored polarization grating profile consists of a spatial modulation of linear and circular birefringences with varying magnitude. From the optical investigation of the recorded grating and exploiting the method reported by Nikolova et al.,[29,30] the amplitudes of the photoinduced linear and circular birefringence modulations have been evaluated as a function of the intensity of the recording beams.

Experimental Section

The polymer used to perform the investigation is a side chain polymethacrylic copolymer with 60 mol % content of oxycyanoazobenzene fragments in the side chains of the macromolecule (Figure 1).[26−28] The synthesis of the copolymer (polymerization degree $\bar{P} = 43$; polydispersity =2.44) is described in refs 27 and 28. The glass transition temperature (T_g) of the polymer is 77 °C. The sample of the polymer was prepared in the form of a 30 μm thick film, placed between two glass plates.

The experimental geometries for holographic recording are reported in Figure 2a. Two linearly polarized coherent beams with equal intensities, from an argon ion laser (Innova 90C, Coherent Inc.) at 514.5 nm, were used for the holographic recording. The beams cross at an angle $2\theta = 5°$, resulting in a spatial periodicity $\Lambda = 6$ μm. With the help of two half-wave plates, the experimental polarization configurations reported in Figure 2b,c have been set up. The polarization states of the two recording beams were set at +45° and −45° with respect to the grating wavevector (along the x-axis) in the first case (Figure 2b) and at 0° and 90° in the second case (Figure 2c).

The typical recoding time is a few seconds, for total recording intensity ranging from 50 to 250 mW/cm^2. Because of the long time stability of the polarization gratings, the analysis of their diffraction properties was performed after the recording process. A linearly polarized probe beam from a He−Ne laser (05-LHP-201, MellesGriot) at 632.8 nm, where the material practically does not absorb, has been used to investigate the gratings features. A rotating analyzer placed on the transmitted probe beams path, between the sample and a photodetector, has been used to characterize the polarization state of the 0, +1, and −1 diffracted order beams, respectively. A rotating half-wave plate before the sample was used to measure the angular dependence of the diffracted beams intensity on the input probe beam polarization direction α, as shown in Figure 2a.

Theoretical Basis

It is well known that the interference pattern of two coherent waves with orthogonal linear polarization results in almost uniform light intensity distribution and periodic polarization state patterns, as those shown in Figure 2b,c.

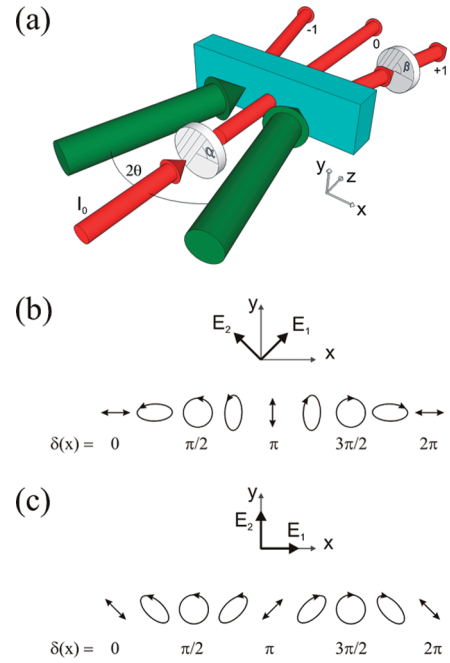

Figure 2. (a) Experimental scheme. The two recording Ar^+ laser beams with linear orthogonal polarization cross at an angle 2θ, while the linearly polarized He−Ne laser probe beam impinges at normal incidence. The angle α is the polarization azimuth of the He−Ne laser probe beam, and β is the angle of the polarization axis of the analyzer. (b and c) Polarization modulations of the interference light field in the two geometries used in the experiment: E_1 and E_2 are the polarization vectors of the two recording waves, and δ is the phase difference between them at a different position (x) along the grating wave vector direction. The recording waves are linearly polarized (b) at ±45° and (c) at 0°/90° with respect to the plane of incidence.

For the experimental geometry with the polarization of the recording waves at ±45°, the Jones vector of the total light field in the superposition region is

$$\vec{E}^{45} = \frac{2}{\sqrt{2}}\begin{pmatrix}\cos\delta/2\\ i\sin\delta/2\end{pmatrix}$$

while in the case with the polarization of the recording waves at 0° and 90°, the Jones vector of the total light field is

$$\vec{E}^{0-90} = \begin{bmatrix}\exp(i\delta)\\ \exp(-i\delta)\end{bmatrix}$$

where $\delta = 2\pi x/\Lambda$ is the phase difference between the two beams and $\Lambda = \lambda/2\sin\theta$ is the spatial periodicity of the polarization grating, 2θ is crossing angle between the two beams, and λ the recording light wavelength.

To study the propagation of the probe light beam through the polarization grating, we used the Jones matrix formalism, as reported in refs 29 and 30. The photosensitive material used in the present work exhibits both photoinduced linear and circular anisotropy, as reported in refs 26−28; then, we consider a nonabsorbing material with photoinduced linear and circular birefringence to evaluate the Jones matrix of the grating. Moreover, we exclude the presence of a superimposed surface relief grating, due to the fact that the polymer film is confined between two glass substrates, and because of the adhesion of the polymer to the glass substrates, the formation of the relief is inhibited.

The Jones matrices of the polarization gratings can be written following the procedure reported in ref 29:

$$\vec{\vec{T}}^{45} = \begin{pmatrix} \cos N + i\Delta\varphi_{\text{lin}} \cos\delta \dfrac{\sin N}{N} & \Delta\varphi_{\text{circ}} \sin\delta \dfrac{\sin N}{N} \\ -\Delta\varphi_{\text{circ}} \sin\delta \dfrac{\sin N}{N} & \cos N - i\Delta\varphi_{\text{lin}} \cos\delta \dfrac{\sin N}{N} \end{pmatrix} \tag{1}$$

when the recording wave polarizations are at +45° and −45° and

$$\vec{\vec{T}}^{0-90} = \begin{pmatrix} \cos N & i\Delta\varphi_{\text{lin}} \cos\delta \dfrac{\sin N}{N} + \Delta\varphi_{\text{circ}} \sin\delta \dfrac{\sin N}{N} \\ i\Delta\varphi_{\text{lin}} \cos\delta \dfrac{\sin N}{N} - \Delta\varphi_{\text{circ}} \sin\delta \dfrac{\sin N}{N} & \cos N \end{pmatrix} \tag{2}$$

when the recording waves polarizations are at 0° and 90°. Here, $\Delta\varphi_{\text{lin}} = \pi\Delta n_{\text{lin}} d/\lambda$, $\Delta\varphi_{\text{circ}} = \pi\Delta n_{\text{circ}} d/\lambda$, and $N = [(\Delta\varphi_{\text{lin}} \cos\delta)^2 + (\Delta\varphi_{\text{circ}} \sin\delta)^2]^{1/2}$, where Δn_{lin} is the photoinduced linear birefringence, Δn_{circ} is the photoinduced circular birefringence, d is the thickness of the polymer film, and λ is the probe light beam wavelength. In the case of small photoinduced optical anisotropies (i.e., $\Delta\varphi_{\text{lin}}$ and $\Delta\varphi_{\text{circ}} \ll 1$), matrices 1 and 2 can be simplified, according to the following approximations: $\cos N \approx 1$ and $\sin N/N \approx 1$. Then, matrices 1 and 2 become equal to:

$$\vec{\vec{T}}^{45} = \begin{pmatrix} 1 + i\Delta\varphi_{\text{lin}} \cos\delta & \Delta\varphi_{\text{circ}} \sin\delta \\ -\Delta\varphi_{\text{circ}} \sin\delta & 1 - i\Delta\varphi_{\text{lin}} \cos\delta \end{pmatrix} \tag{3}$$

and

$$\vec{\vec{T}}^{0-90} = \begin{pmatrix} 1 & i\Delta\varphi_{\text{lin}} \cos\delta + \Delta\varphi_{\text{circ}} \sin\delta \\ i\Delta\varphi_{\text{lin}} \cos\delta - \Delta\varphi_{\text{circ}} \sin\delta & 1 \end{pmatrix} \tag{4}$$

respectively.

Using the Jones formalism, the transmitted fields at 0 and ±1 orders can be easily evaluated from $\vec{E}_{\text{out}} = \vec{\vec{T}}\vec{E}_{\text{in}}$, for a generic linearly polarized probe beam impinging on the grating

$$\vec{E}_{\text{in}} = \begin{pmatrix} \cos\alpha \\ \sin\alpha \end{pmatrix} \tag{5}$$

where α is the azimuth angle. In the case of the ±45° polarization grating, the Jones vectors of the waves diffracted at the ±1 orders and the corresponding normalized intensities are

$$\vec{E}_{\pm1}^{45} = \frac{1}{2}\begin{pmatrix} \Delta\varphi_{\text{lin}} \cos\alpha \mp \Delta\varphi_{\text{circ}} \sin\alpha \\ \pm\Delta\varphi_{\text{circ}} \cos\alpha - \Delta\varphi_{\text{lin}} \sin\alpha \end{pmatrix} \tag{6}$$

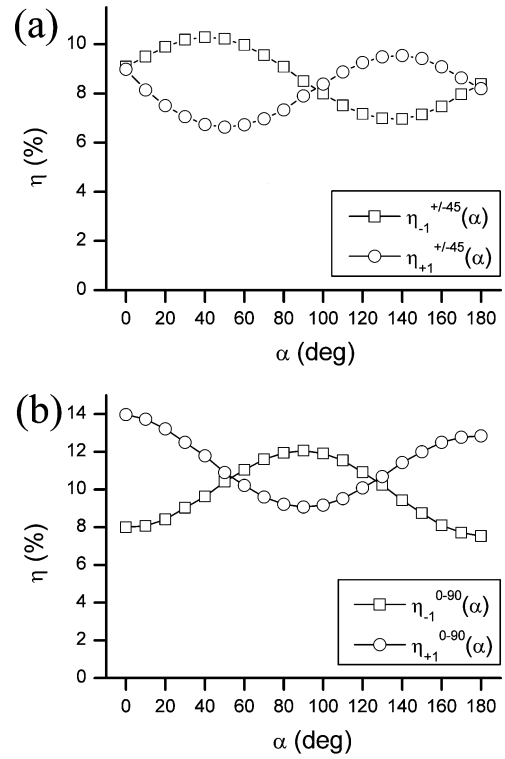

Figure 3. Diffraction efficiency of the waves diffracted in the ±1 orders vs the polarization azimuth α of the He−Ne probe beam for the (a) ±45° and (b) 0−90° polarization gratings.

and

$$\eta_{\pm1}^{45} = \frac{I_{\pm1}^{45}}{I_{\text{in}}} = \frac{1}{4}(\Delta\varphi_{\text{lin}}{}^2 + \Delta\varphi_{\text{circ}}{}^2 \mp \Delta\varphi_{\text{lin}}\Delta\varphi_{\text{circ}} \sin 2\alpha) \tag{7}$$

respectively, where I_{in} is the light intensity of the incident probe beam. The Jones vectors of the beams diffracted at the ±1 orders by the 0−90°polarization grating are

$$\vec{E}_{\pm1}^{0-90} = \frac{1}{2}\begin{bmatrix} (\Delta\varphi_{\text{lin}} \mp \Delta\varphi_{\text{circ}}) \sin\alpha \\ (\Delta\varphi_{\text{lin}} \pm \Delta\varphi_{\text{circ}}) \cos\alpha \end{bmatrix} \tag{8}$$

and the corresponding normalized intensities are

$$\eta_{\pm1}^{0-90} = \frac{I_{\pm1}^{0-90}}{I_{\text{in}}} = \frac{1}{4}(\Delta\varphi_{\text{lin}}{}^2 + \Delta\varphi_{\text{circ}}{}^2 \pm \Delta\varphi_{\text{lin}}\Delta\varphi_{\text{circ}} \cos 2\alpha) \tag{9}$$

In both of the polarization grating configurations, the intensities of the diffracted ±1 orders depend on polarization azimuth α of the impinging probe beam, and eqs 7 and 9 enable evaluation of $\Delta\varphi_{\text{lin}}$ and $\Delta\varphi_{\text{circ}}$ and, therefore, the linear and circular birefringences Δn_{lin} and Δn_{circ} photoinduced in the polymer film.

Results and Discussion

Figure 3a,b shows the dependence of the diffraction efficiencies $\eta_{\pm1}^{45}(\alpha)$ and $\eta_{\pm1}^{0-90}(\alpha)$ as a function of the azimuth angle α of the linearly polarized He−Ne probe beam, for the ±45° and 0−90° polarization grating configurations, respectively. The experimental data refer to polarization gratings recorded with a

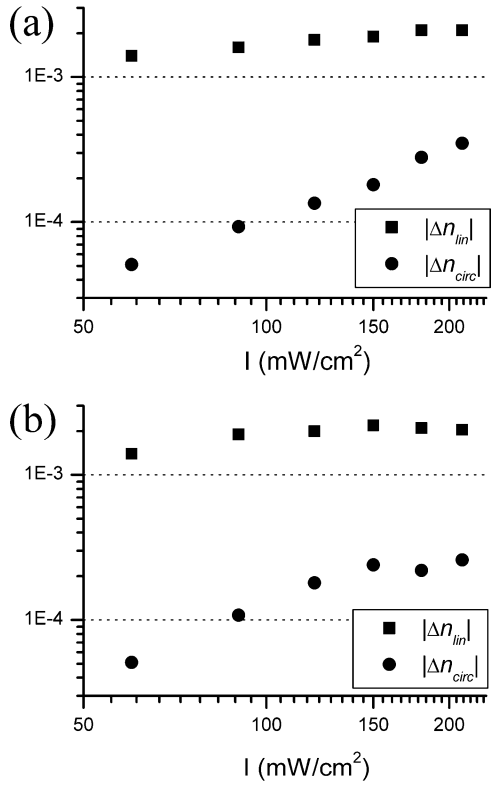

Figure 4. Absolute value of the linear birefringence (solid square) and the circular birefringence (solid circle) vs the total intensity of the recording beams at a fixed exposure time for the (a) ±45° and (b) 0−90° polarization grating configurations.

total intensity of 150 mW/cm^2 and an exposure time of 6 s. The biased harmonic dependence of the diffraction efficiencies of the ±1 orders on the polarization azimuth α is evident for both of the gratings configurations. Also, the maxima and the minima of the $\eta_{\pm1}^{45}(\alpha)$ and $\eta_{\pm1}^{0-90}(\alpha)$ curves correspond with the polarization azimuth of the respective recording beams, as expected from eqs 7 and 9. The values of $\Delta\varphi_{\text{lin}}$ and $\Delta\varphi_{\text{circ}}$ have been evaluated by fitting the experimental data in Figure 3a,b with eqs 7 and 9, and then, the photoinduced linear and circular birefringence Δn_{lin} and Δn_{circ} have been calculated.

In particular, from the experimental data reported in Figure 3a for the ±45° polarization grating and eq 7, we have obtained $|\Delta n_{\text{lin}}| = 1.8 \times 10^{-3}$ and $|\Delta n_{\text{circ}}| = 1.4 \times 10^{-4}$; moreover, Δn_{lin} and Δn_{circ} have the same sign (either both positive or negative). In general, photoinduced linear birefringence in azo-compounds is negative, due to the orientation of the chromophores perpendicular to the light polarization plane. Therefore, we can conclude that both Δn_{lin} and Δn_{circ} are negative, that is, $\Delta n_{\text{lin}} = -1.8 \times 10^{-3}$ and $\Delta n_{\text{circ}} = -1.4 \times 10^{-4}$.

In Figure 4, the absolute values of the photoinduced linear and circular birefringence $|\Delta n_{\text{lin}}|$ and $|\Delta n_{\text{circ}}|$ are reported for increasing total recording intensities, for the ±45° and 0−90° polarization grating configurations. The recording has been performed keeping the exposure time at 6 s and varying the total light intensities in the range 50−210 mW/cm^2. The data reported in the graphs have been obtained by fitting the experimental curves $\eta_{\pm1}^{45}(\alpha)$ and $\eta_{\pm1}^{0-90}(\alpha)$ with eqs 7 and 9.

We observe that while both $|\Delta n_{\text{lin}}|$ and $|\Delta n_{\text{circ}}|$ increase with the recording intensity, $|\Delta n_{\text{circ}}|$ rises much more prominently than $|\Delta n_{\text{lin}}|$, up to 1 order of magnitude in the investigated range of intensity. The mechanism by which the linear birefringence is photoinduced in azo-compounds is well known, and it is based on light-activated *trans*−*cis*−*trans* isomerization cycles of the azo-benzene chromophores, which preferentially orient perpendicularly to the polarization plane of the absorbed light. The concentration of the chromophores aligned perpendicular to the light polarization steadily increases under illumination with polarized light, until a saturation level is attained. A further increase in the irradiation dose, either the intensity and/or the irradiation time, does not induce any significant increase of the photoinduced linear anisotropy. On the other hand, the origin of the photoinduced circular anisotropy, observed when the azo-polymer is irradiated with elliptically or circularly polarized light, is not fully understood at present. Recently, we have proposed[26] that a cooperative motion of the azobenzene chromophors in the same amorphous polymer is responsible for the photoinduced supramolecular chiral structures formation observed upon irradiation with circularly polarized light. The cooperative motion of the side chains of the polymer might explain the more prominent increase in the $|\Delta n_{\text{circ}}|$ with respect to the $|\Delta n_{\text{lin}}|$ curves, at higher intensity. Indeed, the supramolecular scale of the processes involved in the photoinduced circular anisotropy is larger than the molecular level orientation of the azo-chromophores, responsible for the linear anisotropy, and, therefore, would require a greater light dosage before to reach the saturation level.

Finally, we have analyzed the polarization properties of the diffracted beams for both for the ±45° and the 0−90° polarization gratings, recorded at 60 mW/cm^2. In Figure 5, the polar plots of the normalized intensity of the incident and the first-order (+1) beams are reported versus the angle β of the analyzer. The plot of the *s*-polarized incident beam is reported as a reference and has been performed by measuring its intensity after a rotating analyzer, replaced in front of the polymer film. In a similar way, the intensity of the +1 order diffracted beam, for an *s*-polarized probe beam, has been measured versus the azimuth angle β of the analyzer placed on its path, after the grating.

According to Figure 5a, the +1 order beam is linearly polarized, and its azimuth is indistinguishable from the one of incident beam. The experimental data are confirmed by the eq 6 for *s*-polarized incident beam. In this case, in fact, $\alpha = 90°$ and the Jones vectors of the first ±1 orders are

$$E_{\pm1}^{45} = \frac{1}{2}\begin{pmatrix} \mp\Delta\varphi_{\text{circ}} \\ -\Delta\varphi_{\text{lin}} \end{pmatrix} \tag{10}$$

The diffracted beams preserve the linear polarization state; moreover, because $|\Delta\varphi_{\text{lin}}|$ at the recording intensity of 60 mW/cm^2 is 1 order of magnitude higher than $|\Delta\varphi_{\text{circ}}|$, also the azimuth angles do not change significantly (∼85°). The measurements presented in Figure 5b refer to the 0−90° geometry. The incident probe beam is still *s*-polarized, then $\alpha = 90°$, and the Jones vectors of the ±1 orders predicted by eq 8 are

$$E_{\pm1}^{0-90} = \frac{1}{2}\begin{bmatrix} (\Delta\varphi_{\text{lin}} \mp \Delta\varphi_{\text{circ}}) \\ 0 \end{bmatrix} \tag{11}$$

For both of the ±1 orders, the expected polarization is linear and horizontal, that is, orthogonal with respect to the incident wave, regardless of relative magnitude of $|\Delta\varphi_{\text{lin}}|$ and $|\Delta\varphi_{\text{circ}}|$. The difference is only on the amplitudes of the diffracted fields and then on the diffraction efficiency of the −1 and +1 orders. The experimental results show that the diffracted +1 beam preserves the linear polarization, and it is almost perpendicular with respect to the incident one.

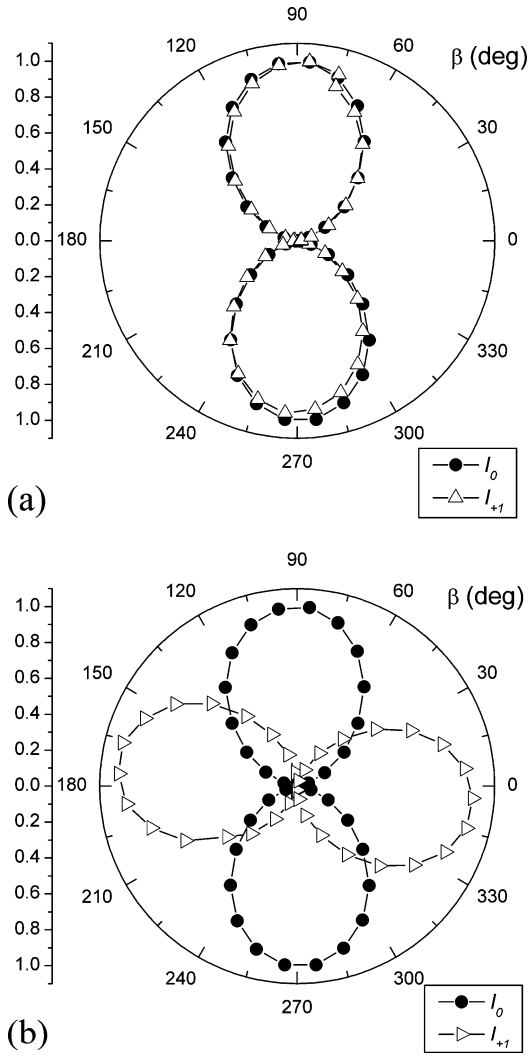

Figure 5. Polar plot of the incident (solid circle) and first-order (open triangle) diffracted waves of the probe beams for the (a) ±45° and (b) 0−90° polarization grating configuration.

In all cases, the recorded structures have long time stability and full reconfigurability. The grating can be erased, increasing the temperature above the glass transition temperature or even by an uniform light irradiation, and written again several times preserving their features.

Conclusions

We report the experimental investigation on polarization holographic recording in an amorphous and nonchiral azocopolymer. The reported results show that the amorphous polymeric film undergoes a light-guided inhomogeneous structural modification after illumination with proper polarized light pattern, including linear, elliptical, and circular polarization. The recorded structures depend on the chirality of the light and are compatible with a light-induced modification of the polymer structure at the supramolecular level, including circular and linear anisotropy. A proper optical characterization of the recorded holograms enables measurement of the photoinduced linear and circular birefringence. The different scales of the photoinduced processes originating the linear and circular anisotropies are responsible for the different growth rate of the $|\Delta n_{lin}|$ and $|\Delta n_{circ}|$ versus the recording intensity. The reported results together with the high spatial resolution, the long time stability, and the full reconfigurability, guaranteed by the intrinsic reversibility of the photoinduced processes and by the polymer features, make it a good candidate for reconfigurable 2D or 3D structured materials with versatile architecture of the anisotropy and the chirality.

Acknowledgment. We deeply thank Dr. Sergey Kostromin for the synthesis of copolymer and its characterization. This work was partially supported by MIUR (PRIN 2007), Licryl-CNR, CEMIF.CAL, and the Russian Foundation for basic Research (Projects 08-03-00481 and 09-03-12234).

References and Notes

(1) Nikolova, L.; Todorov, T. *Opt. Acta* **1984**, *31*, 579–588. Nikolova, L.; Ramanujam, P. S. *Polarization Holography*; Cambridge University Press: Cambridge, 2009.
(2) Samorì, P.; Cacialli, F.; Anderson, H. L.; Rowan, A. E. *Adv. Mater.* **2006**, *18*, 1235–1238.
(3) Barth, J. V.; Costantini, G.; Kem, K. *Nature* **2005**, *437*, 671–679.
(4) Kocer, A.; Walko, M.; Meijberg, W.; Feringa, B. L. *Science* **2005**, *309*, 755–758.
(5) Berkovuch, G.; Krongauz, V.; Weiss, V. *Chem. Rev.* **2000**, *100*, 1741–1753.
(6) Delaire, J. A.; Nakatani, K. *Chem. Rev.* **2000**, *100*, 1817–1845.
(7) Ikeda, T.; Tsutsumi, O. *Science* **1995**, *268*, 1873–1875.
(8) Irie, M. *Chem. Rev.* **2000**, *100*, 1683–1684.
(9) Bobrovsky, A.; Shibaev, V. P. *Polymer* **2006**, *47*, 4310–4317.
(10) Shibaev, V. P. *Polym. Sci. A* **2009**, *51*, 1131–1193.
(11) Fukuda, T.; Kim, J. Y.; Barada, D.; Yase, K. *J. Photochem. Photobiol., A* **2006**, *183*, 273–279.
(12) Tejedor, R. M.; Millaruelo, M.; Oriol, L.; Serrano, J. L.; Alcalà, R.; Rodrýguez, F. J.; Villacampa, B. *J. Mater. Chem.* **2006**, *16*, 1674–1680.
(13) Natansohn, A.; Rochon, P. *Chem. Rev.* **2002**, *102*, 4139–4175.
(14) Yager, K. G.; Barrett, C. J. *J. Photochem. Photobiol., A* **2006**, *182*, 250–261.
(15) Todorov, T.; Nikolova, L.; Tomova, N. *Appl. Opt.* **1984**, *23*, 4309–4312.
(16) Kim, M. J.; Yoo, S. J.; Kim, D. Y. *Adv. Funct. Mater.* **2006**, *16*, 2089–2094.
(17) Tamaoki, N.; Wada, M. *J. Am. Chem. Soc.* **2006**, *128*, 6284–6285.
(18) Choi, S. W.; Kawauchi, S.; Ha, N. Y.; Takezoe, H. *Phys. Chem. Chem. Phys.* **2007**, *9*, 3671–3681.
(19) Pagès, S.; Lagugné-Labarthet, F.; Buffeteau, T.; Sourisseau, C. *Appl. Phys. B: Laser Opt.* **2002**, *75*, 541–548.
(20) Nedelchev, L.; Nikolova, L.; Todorov, T.; Petrova, T.; Tomova, N.; Dragostinova, V.; Ramanujam, P. S.; Hvilsted, S. *J. Opt. A: Pure Appl. Opt.* **2001**, *3*, 304–310.
(21) Nikolova, L.; Nedelchev, L.; Todorov, T.; Petrova, T.; Tomova, N.; Dragostinova, V. *Appl. Phys. Lett.* **2000**, *77*, 657–659.
(22) Sumimura, H.; Fukuda, T.; Kim, J. Y.; Barada, D.; Itoh, M.; Yatagai, T. *Jpn. J. Appl. Phys., Part 1* **2006**, *45*, 451–455.
(23) Iftime, G.; Lagugné-Labarthet, F.; Natansohn, A.; Rochon, P. *J. Am. Chem. Soc.* **2000**, *122*, 12646–12650.
(24) Choi, S. W.; Ha, N. Y.; Shiromo, K.; Rao, N. V. S.; Paul, M. Kr.; Toyooka, T.; Nishimura, S.; Wu, J. W.; Park, B.; Takanishi, Y.; Ishikawa, K.; Takezoe, H. *Phys. Rev. E* **2006**, *73*, 021702.
(25) Kawamoto, M.; Sassa, T.; Wada, T. *J. Phys. Chem. B* **2010**, *114*, 1227–1232.
(26) Cipparrone, G.; Pagliusi, P.; Provenzano, C.; Shibaev, V. P. *Macromolecules* **2008**, *41*, 5992–5996.
(27) Belayev, S.; Zvetkova, T.; Panarin, Yu.; Kostromin, S.; Shibaev, V. *Vysokomolek. Soedin., Seris B* **1986**, *28*, 789–793.
(28) Simonov, A. N.; Uraev, D. V.; Kostromin, S. G.; Shibaev, V. P.; Stakhanov, A. I. *Laser Phys.* **2002**, *12*, 1294–1302.
(29) Nikolova, L.; Todorov, M. I.; Andruzzi, F.; Hvilsted, S.; Ramanujam, P. S. *Appl. Opt.* **1996**, *35*, 3835–3840.
(30) Naydenova, L.; Nikolova, L.; Todorov, M. I.; Holme, N. C. R.; Hvilsted, S.; Ramanujam, P. S. *J. Opt. Soc. Am.* **1998**, *15*, 1257–1265.

JP103899B